CARBON 50 (2012) 2220–2225

Available at www.sciencedirect.com

SciVerse ScienceDirect

journal homepage: www.elsevier.com/locate/carbon

Mechanical measurements of ultra-thin amorphous carbon membranes using scanning atomic force microscopy

Ji Won Suk, Shanthi Murali, Jinho An, Rodney S. Ruoff *

Department of Mechanical Engineering and the Materials Science and Engineering Program, The University of Texas at Austin, One University Station C2200, Austin, TX 78712-0292, United States

ARTICLE INFO

Article history:
Received 21 October 2011
Accepted 11 January 2012
Available online 20 January 2012

ABSTRACT

The elastic modulus of ultra-thin amorphous carbon films was investigated by integrating atomic force microscopy (AFM) imaging in contact mode with finite element analysis (FEA). Carbon films with thicknesses of ~10 nm and less were deposited on mica by electron beam evaporation and transferred onto perforated substrates for mechanical characterization. The deformation of these ultra-thin membranes was measured by recording topography images at different normal loads using contact mode AFM. The obtained force-distance relationship at the center of membranes was analyzed to evaluate both the Young's modulus and pre-stress by FEA. From these measurements, Young's moduli of 178.9 ± 32.3, 193.4 ± 20.0, and 211.1 ± 44.9 GPa were obtained for 3.7 ± 0.08, 6.8 ± 0.12, and 10.4 ± 0.17 nm thick membranes, respectively. Raman spectroscopy, X-ray photoelectron spectroscopy, and transmission electron microscopy were used for characterizing the chemical and structural properties of the films, including the content of sp^2 and sp^3 hybridized carbon atoms.

1. Introduction

Amorphous carbon (a-C) is a disordered phase of carbon without long-range order, containing carbon atoms mostly in graphite-like sp^2 and diamond-like sp^3 hybridization sites. Depending on the relative concentrations of sp^2 or sp^3 hybridized carbon, a-C has shown excellent physical properties such as high hardness, low friction coefficient, chemical inertness, relatively high thermal conductivity, and optical transparency [1]. Electron beam evaporation has been used for fabricating uniform thin carbon films along with other deposition methods including chemical vapor deposition and sputtering. However, reports on the mechanical properties of electron beam evaporated carbon films are few [2].

Mechanical properties of a-C films have been investigated with various approaches such as nanoindentation and surface Brillouin scattering (SBS). Nanoindentation measurements provide the hardness, and the reduced Young's modulus ($E_r = E/(1-\nu^2)$, where E is the Young's modulus and ν is the Poisson's ratio) can be derived from the indentation curve. However, the nanoindentation technique is highly sensitive to the substrate properties: the contact depth should be less than 10–20% of the film thickness to avoid the substrate effect [3]. In addition, the hardness and Young's modulus values extracted from nanoindentation measurements can depend significantly on whether the shape of the blunt tip and the substrate effect were taken into account [4]. SBS can provide nondestructive measurements of the elastic constants of thin films with thicknesses less than 10 nm [5]. In principle, SBS measures the velocities of surface acoustic waves along the thin films. If the film thickness and mass density are measured independently, the elastic constants can be derived from measured acoustic velocities [6]. However, additional measurements are needed for characterizing the density of

* *Corresponding author.*
E-mail address: r.ruoff@mail.utexas.edu (R.S. Ruoff).
0008-6223/$ - see front matter
doi:10.1016/j.carbon.2012.01.037

ultra-thin films. Recently, atomic force microscopy (AFM) imaging in contact mode was used to measure elastic modulus of suspended atomically-thin (monolayer graphene oxide) membranes [7]. Therefore, it can also be a reliable alternative to nanoindentation or SBS for measuring the elastic modulus of ultra-thin a-C films.

Herein, we used the contact mode AFM measurements on suspended a-C membranes to characterize the mechanical properties of ultra-thin a-C films fabricated by electron beam evaporation. The structural deformation of the membrane was measured by scanning an AFM tip over the membrane at various normal loads. The obtained deformation profiles of the membrane as a function of the applied loads were analyzed by finite element analysis (FEA) to extract both the Young's modulus and pre-stress. Raman spectroscopy, X-ray photoelectron spectroscopy (XPS), and high magnification transmission electron microscopy (TEM) were used to characterize the structural and chemical properties of the a-C films.

2. Experimental

Carbon films were deposited on freshly cleaved mica at room temperature by electron beam evaporation (MED 020 high vacuum coating system, BAL-TEC). The evaporation was done at high vacuum ($\leqslant 10^{-6}$ mbar) by heating a tungsten filament. Electrons emitted from the heated tungsten filament were accelerated with high voltage and impinged on a graphite source, which evaporated carbon atoms. The carbon films of various thicknesses were made by controlling the deposition time at room temperature. To measure the thicknesses of the films, each film was transferred onto cleaved mica and the thickness was measured at cracks through the film by contact mode AFM (model CP, Park Scientific Instrument).

The structural and chemical properties of the carbon films were analyzed by Raman spectroscopy (488 nm excitation laser, 100× objective lens, WITec Alpha 300 micro-Raman imaging system) and XPS (Kratos AXIS Ultra DLD spectrometer, monochromated Al Kα emission at 1486.6 eV with an operating power of 150 W) on the as-prepared samples on mica. Charge neutralizer was used during the XPS measurement and the C 1 s peak was shifted with center at 284.5 eV. Atomic structures of the films were observed by TEM (JEOL 2010F) imaging and selected area electron diffraction (SAED) patterns after transferring the film on perforated silicon nitride supporting film TEM grids (Ted Pella).

In order to characterize the mechanical properties, the carbon films were transferred onto a silicon nitride TEM grid having 2.8 μm diameter holes. The carbon film on mica was slowly inserted into distilled water at an angle. While the substrate was being immersed into water, the carbon film was delaminated from mica and floated onto the water surface. The TEM grid was then placed on the bottom of the water bath, and the film was lowered down to the grid by pulling out water from the bath. The carbon film on the grid was dried under vacuum overnight.

The Young's modulus and pre-stress of carbon films were characterized on suspended carbon membranes by using contact mode AFM and FEA. Several topography images were obtained by scanning the membrane at various applied loads. The line profiles at the center of the membrane were extracted as a function of the applied loads from the recorded topography images, which generated the force-distance relationship at the center of the membrane. FEA was used to make a map of the calculated displacements with assumed Young's modulus and pre-stress of the membrane. The ANSYS Parametric Design Language (APDL) was used to model the contact between the AFM tip and the membrane with varying assumed values of the Young's moduli and pre-stresses. A 2-node shell element was used for axisymmetric analysis of the membrane. The AFM tip was modeled as a hemisphere with a radius of 23.7 nm (measured by TEM) and the material properties of silicon nitride. The contact between the tip and membrane was assumed to be frictionless. The membrane was assumed to be isotropic. Center displacements at a given applied load were calculated with various Young's moduli and pre-stresses by FEA. When the measured displacement at a given load was equal to the calculated displacement, we could obtain infinite pairs of possible Young's moduli and pre-stresses. These pairs of values formed a line when they were plotted in a two-dimensional (2D) map with the Young's modulus (ordinate) and pre-stress (abscissa). By repeating this analysis for other given loads, we could obtain other lines with different slopes in the map. Therefore, the overlapped area provided the most possible values of the Young's modulus and pre-stress of the membrane. The detailed procedure has been described previously [7]. The Poisson's ratio was assumed to be 0.25 in our analysis [8].

3. Results and discussion

Three carbon films were deposited on mica with three different thicknesses. The thicknesses were measured in several areas and the average values were 3.7 ± 0.08, 6.8 ± 0.12, and 10.4 ± 0.17 nm. Fig. 1a shows a scanning electron microscopy (SEM, Quanta F600 ESEM, FEI) image of a 3.7 nm thick film over a perforated silicon nitride supporting film with 2.8 μm diameter holes. The wrinkle on the bottom right corner indicates that the holes of the supporting film were covered by the ultra-thin carbon film. An AFM topography image (Fig. 1b) confirmed that the film was freely suspended over the holes and individual membranes did not have any wrinkles or folds. Fig. 1c and d shows a high magnification TEM image and the SAED pattern of the suspended carbon film. Only an amorphous granular structure with diffuse hallows in SAED was observed in the carbon films. Raman spectra of all films showed broad, asymmetric bands at 900–1800 cm^{-1}, which indicated that the deposited carbon film was amorphous (Fig. 1e) [9,10]. The broad band could be deconvoluted into two characteristic peaks, which are the D and G bands. The D band was positioned at ~1383 cm^{-1} with a full width at half maximum (FWHM) of ~302 cm^{-1}, while the G band was positioned at ~1556 cm^{-1} with a FWHM of ~140 cm^{-1}. The integrated intensity ratio of D band to G band, I_D/I_G, was ~1.14. The other films having 6.8 and 10.4 nm thicknesses showed similar Raman characteristics with I_D/I_G of ~2.14 and ~2.21, respectively. It is known that there can be a correlation between the I_D/I_G and the diameter of graphitic clusters L_a. Tuinstra and Koenig noted that the I_D/I_G varies

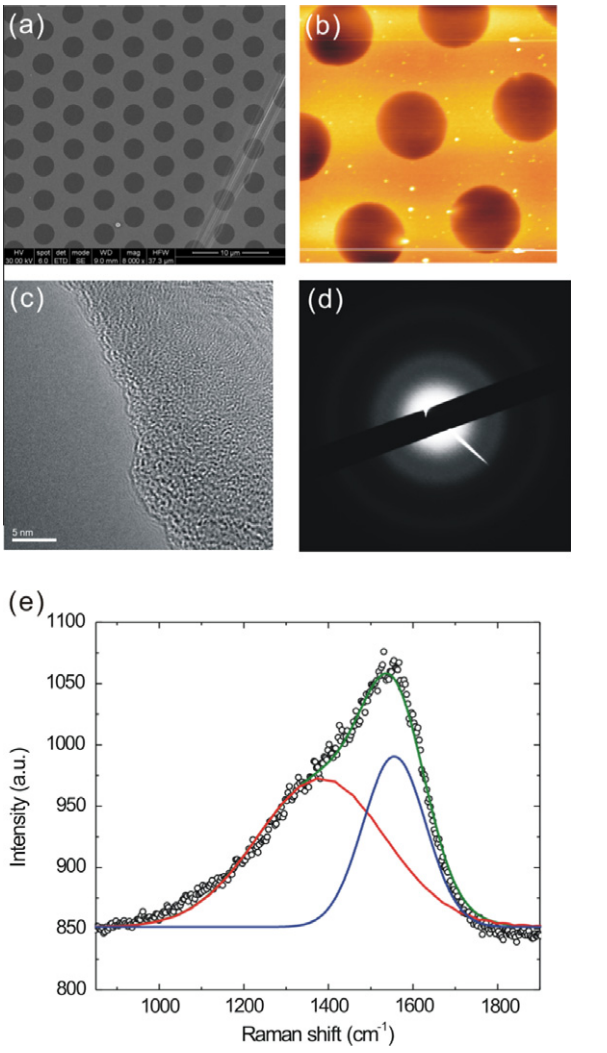

Fig. 1 – (a and b) SEM and AFM topography images of a 3.7 nm thick a-C film spanning over perforated holes. The AFM image was taken from an area of $10 \times 10\ \mu m^2$. (c and d) High magnification TEM image and SAED pattern of the 3.7 nm thick a-C film. (e) Raman spectra of the 3.7 nm thick a-C film on mica. The circles represent the experimental data. The blue and red lines are deconvoluted Gaussian peaks. The green solid line is the resultant of the deconvoluted peaks. (For interpretation of the references to colour in this figure legend, the reader is referred to the web version of this article.)

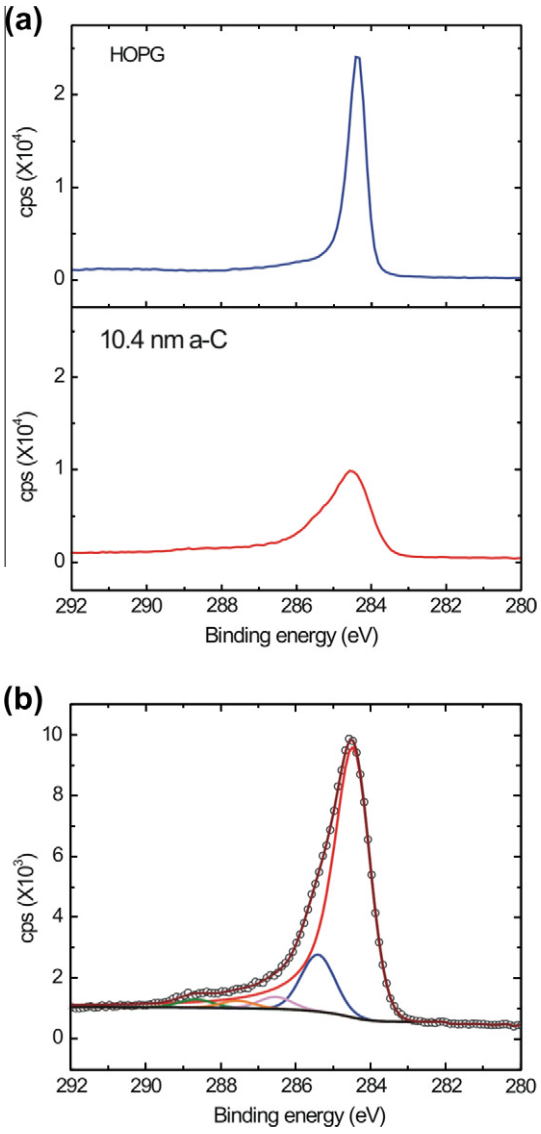

Fig. 2 – (a) Comparison of the C 1 s peaks from XPS spectra for HOPG and a 10.4 nm thick a-C film on mica. (b) Deconvolution of the C 1 s spectrum for the 10.4 nm thick a-C film. The circles represent experimental data. The black solid line is the Shirley background and other solid lines represent five deconvoluted peaks. The brown solid line is the resultant of the deconvoluted peaks. (For interpretation of the references to colour in this figure legend, the reader is referred to the web version of this article.)

inversely with L_a [11]. However, this relationship holds for graphite and nanocrystalline graphite, but does not remain valid for a-C. Ferrari and Robertson suggested that for L_a below 2 nm, the ratio increases proportionally with L_a^2 [12]. Thus, the variation of I_D/I_G of the electron beam evaporated a-C films indicates that there can be a change in the chemical structure of each film, which may affect the mechanical properties.

Further analysis was performed by XPS on the a-C films on mica. Fig. 2a shows the comparison of the C 1 s peaks of a 10.4 nm thick a-C film and highly ordered pyrolytic graphite (HOPG). As reported in previous work [13–15], the C 1 s core-level spectrum of the a-C film showed a broad peak comprised of the binding energies of graphite and diamond. The C 1 s core-level spectrum could be deconvoluted into five contributions with binding energies of 284.5, 285.4, 286.5, 287.6, and 288.7 eV. The background signal was subtracted by using a Shirley background. The decompositions were obtained using an asymmetric peak analogous to that observed for graphite shown in Fig. 2a [16]. The shapes of the remaining peaks were assumed to be 20% Lorentzian and 80% Gaussian [15]. The

main peak at 284.5 eV was assigned to sp^2-hybridized graphite-like carbon atoms. The peak at 285.4 eV is thought to originate from sp^3-hybridized carbon atoms as in diamond-like carbon. This is accordance with the shift of ~0.9 eV between the C 1 s core levels of diamond and graphite [13]. The remaining peaks correspond to carbon atoms in various functional groups: C–O (286.6 eV), C═O (287.2 eV), and O–C═O (288.8 eV) [14,17–19]. The oxygen in the a-C films might be due to the surface chemisorption of water and oxygen in air. It has been reported that the relative amounts of carbon atoms of each bonding type can be determined by integrating the areas of the sp^2 and sp^3 peaks and comparing them [13,14]. Table 1 shows relative amounts of the sp^2 and sp^3 hybridized carbon in the three films, as interpreted from the XPS data. The relative atomic amounts of sp^3 hybridized carbon increased slightly from 12.8% to 16.1% as the thickness increased from 3.7 to 10.4 nm. On the basis of high magnification TEM, Raman spectroscopy, and XPS characterization, the a-C films had ~12–16% sp^3 hybridization carbon contents.

Mechanical properties of the a-C films, including the Young's modulus and pre-stress, were investigated for the three different films by the combination of AFM tests and FEA. Fig. 3a and b shows 3D topography images of a 3.7 nm thick membrane at 0 and 24.2 nN. Line profiles passing through the center of the membrane were obtained from the topography images with increasing applied loads as shown in Fig. 3c. The membrane was stuck to the side wall of the hole at zero applied load due to the van der Waals interaction. The adhesion depth of the membrane to the sidewall decreased from ~5 to ~1 nm as the thickness of the films increased.

In the mechanical characterization of thin membranes, the pre-stress is an important parameter since the out-of-plane deformation is strongly affected by the pre-stress of the membrane [20]. Therefore, the pre-stress should be considered during the evaluation of the Young's modulus of the membrane. The last four applied loads were analyzed with the measured center displacements for extracting both the Young's modulus and pre-stress of the membrane. For example, for the 3.7 nm thick membrane shown in Fig. 3, the center displacements were 15.5, 19.6, 22.9, and 26.2 nm for the applied loads of 12.1, 16.1, 20.2, and 24.2 nN, respectively. At each given load, the center displacements were calculated by FEA with various Young's moduli and pre-stresses. Possible pairs of the Young's moduli and pre-stresses were extracted by matching the calculated displacements with the measured one. Those pairs formed a line at a given load as shown in Fig. 4. This process was repeated for the remaining three applied loads and plotted in the same map (Fig. 4). Therefore, the overlapped area of the four lines represents the most possible pairs of the Young's moduli and pre-stresses of the membrane. Every point in the overlapped area was averaged to get the mechanical properties of the membrane.

Fig. 5 shows the mechanical properties of the a-C membranes with three different thicknesses. The Young's moduli of the a-C membranes with 3.7 ± 0.08, 6.8 ± 0.12, and 10.4 ± 0.17 nm thicknesses were 178.9 ± 32.3, 193.4 ± 20.0, and 211.1 ± 44.9 GPa, respectively. The mechanical properties of a-C films have been known to change over a wide range with their chemical and structural properties such as sp^2 and sp^3 carbon contents. The constraint-counting theory of the elastic properties of random covalent networks [21] predicts that the Young's modulus should depend on mean-atomic coordination Z as $E = E_0(Z\text{-}2.4)^{1.5}$ where $E_0 = 435$ GPa. At $Z = 2.4$, the networks have zero rigidity, which means that there is a transition from a floppy structure to a more rigid structure. The mean coordination Z is given by the sp^3 fraction, x, as $Z = 3 + x$ [5,22]. This prediction provided a reasonable estimate of the Young's modulus of a-C films as a function of the sp^3 carbon content. For example, the Young's modulus for the tetrahedral amorphous carbon (ta-C) film with 88% sp^3 carbon as measured by SBS was 757 GPa [5], which is close to the calculated value from the equation of 783 GPa. The Young's moduli calculated by the theoretical model with the experimentally-measured fraction of sp^3 carbon (as measured by XPS) showed slightly higher values than the experimental results for the moduli (Fig. 5a). The calculated Young's moduli of the a-C membranes were 270.2, 275.6, and 288.8 GPa for membranes of 3.7, 6.8, and 10.4 nm thickness, respectively. The theoretical model essentially assumes that the carbon film does not contain any hydrogen and clustering. It is known that hydrogen content in a-C films can strongly reduce its network rigidity [5,22]. For example, ta-C films with a high sp^3 carbon content of 88% showed a Young's modulus of 757 GPa, while hydrogenated tetrahedral amorphous carbon (ta-C:H) with 70% sp^3 carbon and 30% hydrogen had a Young's modulus of 300 GPa [5]. In this respect, the lower Young's moduli of the a-C films characterized in this work might be attributed to a slight amount of hydrogen incorporated into the films.

The sp^2/sp^3 ratio is another indicator of the chemical structure of a-C films and mechanical properties of a-C films can be evaluated in terms of the sp^2/sp^3 ratio. It has been reported that the elastic modulus of argon-diluted diamond-like carbon films increased from 100.0 to 202.5 GPa as the sp^3/sp^2 ratio increased from 1.5 to 2.4 and the sp^3 fraction

Table 1 – sp^2 and sp^3 hybridized carbon in a-C films as analyzed from the C 1 s XPS spectra.

Thickness (nm)	sp^2 C		sp^3 C		sp^2/sp^3
	Peak position (eV)	Amount (%)	Peak position (eV)	Amount (%)	
3.7	284.5	77.0	285.4	12.8	6.01
6.8	284.5	76.3	285.4	13.8	5.53
10.4	284.5	76.1	285.4	16.1	4.73

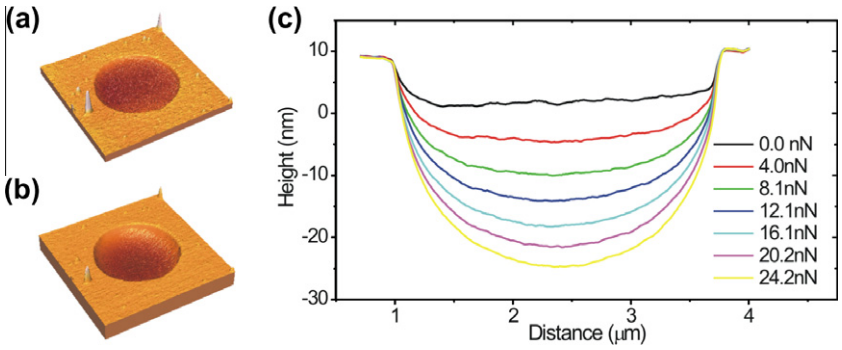

Fig. 3 – (a and b) 3D AFM topography images of a 3.7 nm thick a-C membrane at two different loads of 0.0 and 24.2 nN. (c) Cross-sectional line profiles at the center of the scanned membrane at varying normal loads.

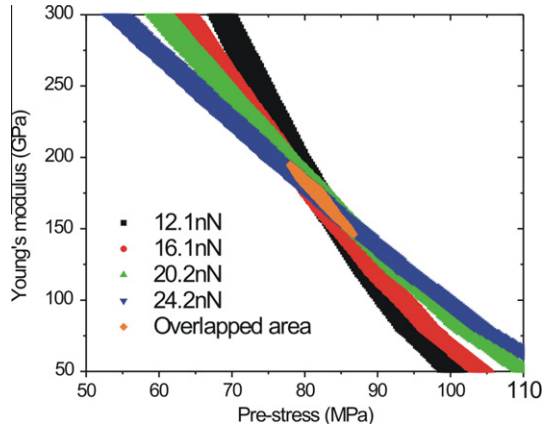

Fig. 4 – 2D elastic modulus versus pre-stress map obtained from four different normal loads for the membrane shown in Fig. 3.

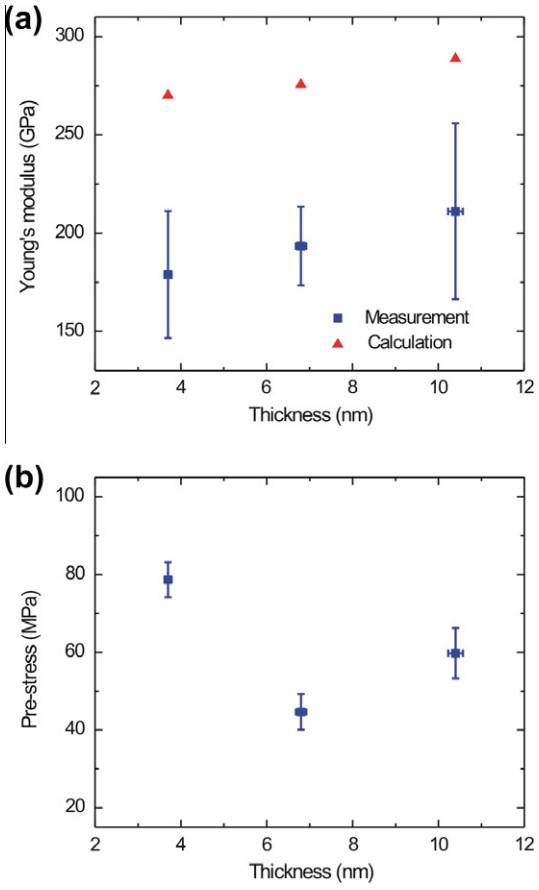

Fig. 5 – (a) Young's moduli and (b) pre-stresses of the a-C membranes as a function of the film thicknesses.

increased from 39.4% to 49.5% [14]. In our work, the sp^2/sp^3 ratio decreased as the thickness of the films increased as shown in Table 1. Therefore, the slight increase of the average Young's modulus might be correlated to the decrease of the sp^2/sp^3 ratio along with an increase in the sp^3 fraction.

The pre-stress of the membrane was simultaneously obtained from the measurement and analysis as shown in Fig. 5b. The pre-stresses of the membranes were 78.6 ± 4.5, 44.7 ± 4.6, and 59.8 ± 6.5 MPa for the 3.7 ± 0.08, 6.8 ± 0.12, and 10.4 ± 0.17 nm thick membranes, respectively. The order of magnitude of the pre-stress is close to that of the carbon membranes made by the same water-based transfer technique [7]. This is due to the stretching of the film caused by the surface tension of water during the transfer of the film onto the perforated substrate. In addition, the adhesion of the film to the sidewall of the holes may also attribute to the pre-stress of the suspended membranes. The 3.7 nm thick a-C film adhered to the sidewall to a depth of ~5 nm, and the 6.8 and 10.4 nm thick films to a depth of ~1–2 nm. This rationalizes the 3.7 nm thick a-C membrane having the highest pre-stress compared to the other two films.

4. Conclusions

In this work, ultra-thin a-C films deposited by electron beam evaporation were mechanically characterized with a new approach which combines scanning AFM with FEA. The nanometer-thick membranes made of the deposited a-C showed average Young's moduli from ~178 to ~211 GPa, with the modulus increasing with the membrane thickness. XPS characterization showed that the sp^3 hybridized carbon content increased slightly as the thickness increased. Therefore, the slight increase of the Young's moduli might be due to the change in the sp^3 carbon content in the a-C films as predicted by theoretical calculations. This mechanical measurement provides the elastic properties of electron beam

deposited thin a-C films as well as an alternative method to characterize the ultra-thin membranes.

Acknowledgment

This work was supported by the NSF (#0969106; CMMI: Mechanical Characterization of Atomically Thin Membranes).

REFERENCES

[1] Grill A. Diamond-like carbon: state of the art. Diam Relat Mater 1999;8(2–5):428–34.
[2] Logothetidis S, Charitidis C, Patsalas R. Engineering properties of fully sp^3- to sp^2-bonded carbon films and their modifications after post-growth ion irradiation. Diam Relat Mater 2002;11(3–6):1095–9.
[3] Li XD, Bhushan B. A review of nanoindentation continuous stiffness measurement technique and its applications. Mater Charact 2002;48(1):11–36.
[4] Lemoine P, Quinn JP, Maguire PD, Zhao JF, McLaughlin JA. Intrinsic mechanical properties of ultra-thin amorphous carbon layers. Appl Surf Sci 2007;253(14):6165–75.
[5] Ferrari AC, Robertson J, Beghi MG, Bottani CE, Ferulano R, Pastorelli R. Elastic constants of tetrahedral amorphous carbon films by surface Brillouin scattering. Appl Phys Lett 1999;75(13):1893–5.
[6] Beghi MG, Ferrari AC, Bottani CE, Libassi A, Tanner BK, Teo KBK, et al. Elastic constants and structural properties of nanometre-thick diamond-like carbon films. Diam Relat Mater 2002;11(3–6):1062–7.
[7] Suk JW, Piner RD, An J, Ruoff RS. Mechanical properties of monolayer graphene oxide. ACS Nano 2010;4(11):6557–64.
[8] Marques FC, Lacerda RG, Champi A, Stolojan V, Cox DC, Silva SRP. Thermal expansion coefficient of hydrogenated amorphous carbon. Appl Phys Lett 2003;83(15):3099–101.
[9] Chu PK, Li LH. Characterization of amorphous and nanocrystalline carbon films. Mater Chem Phys 2006;96(2–3):253–77.
[10] Rao J, Lawson KJ, Nicholls JR. The characterisation of e-beam evaporated and magnetron sputtered carbon films fabricated for atomic oxygen sensors. Surf Coat Tech 2005;197(2–3):154–60.
[11] Tuinstra F, Koenig JL. Raman spectrum of graphite. J Chem Phys 1970;53(3):1126–30.
[12] Ferrari AC, Robertson J. Interpretation of Raman spectra of disordered and amorphous carbon. Phys Rev B 2000;61(20):14095–107.
[13] Haerle R, Riedo E, Pasquarello A, Baldereschi A. Sp^2/sp^3 hybridization ratio in amorphous carbon from C 1 s core-level shifts: X-ray photoelectron spectroscopy and first-principles calculation. Phys Rev B 2001;65(4):045101.
[14] Dwivedi N, Kumar S, Malik HK, Govind, Rauthan CMS, Panwar OS. Correlation of sp^3 and sp^2 fraction of carbon with electrical, optical and nano-mechanical properties of argon-diluted diamond-like carbon films. Appl Surf Sci 2011;257(15):6804–10.
[15] Leung TY, Man WF, Lim PK, Chan WC, Gaspari F, Zukotynski S. Determination of the sp^3/sp^2 ratio of a-C:H by XPS and XAES. J Non-Cryst Solids 1999;254:156–60.
[16] Diaz J, Paolicelli G, Ferrer S, Comin F. Separation of the sp^3 and sp^2 components in the C 1 s photoemission spectra of amorphous carbon films. Phys Rev B 1996;54(11):8064–9.
[17] Stankovich S, Piner RD, Chen XQ, Wu NQ, Nguyen ST, Ruoff RS. Stable aqueous dispersions of graphitic nanoplatelets via the reduction of exfoliated graphite oxide in the presence of poly(sodium 4-styrenesulfonate). J Mater Chem 2006;16(2):155–8.
[18] Tseng WS, Tseng CY, Kuo CT. Effects of gas composition on highly efficient surface modification of multi-walled carbon nanotubes by cation treatment. Nanoscale Res Lett 2009;4(3):234–9.
[19] Chen XQ, Xu ZH, Li XD, Shaibat MA, Ishii Y, Ruoff RS. Structural and mechanical characterization of platelet graphite nanofibers. Carbon 2007;45(2):416–23.
[20] Tabata O, Kawahata K, Sugiyama S, Igarashi I. Mechanical property measurements of thin-films using load deflection of composite rectangular membranes. Sensor Actuator 1989;20(1–2):135–41.
[21] He H, Thorpe MF. Elastic Properties of Glasses. Phys Rev Lett 1985;54(19):2107–10.
[22] Schultrich B, Scheibe HJ, Grandremy G, Drescher D, Schneider D. Elastic modulus as a measure of diamond likeness and hardness of amorphous carbon films. Diam Relat Mater 1996;5(9):914–8.